At 120–150 g/cm² atmospheric depth (about the depth of the Pfotzer maximum) the efficiency drops to 70 percent with bias "0." This is interpreted as being caused by particles of velocity below the Čerenkov threshold ($\beta=0.7$ for lucite) which trigger the telescope but do not give a detectable Čerenkov pulse. Analysis shows that these particles must be protons, as mesons or electrons having the 25 g/cm² range necessary to traverse the detector would be well above the threshold. Comparison with the sea-level data shows that between 24 percent and 30 percent of the particles at the Pfotzer maximum having a range of 25 g/cm² or greater must be these protons, of energy between 185 and 400 Mev. The absolute flux is 0.07 ± 0.01 particle cm^{-2} sec^{-1} sterad^{-1}.

At 17 g/cm² atmospheric depth the vertical efficiency is 93 percent, indicating that, as in the basement laboratory, all or nearly all particles are relativistic with β well above 0.7. At 60° zenith angle, however, the nonrelativistic or backward flux increases, and the efficiency drops to 69 percent. If one assumes that the relativistic vertical backward flux at sea level or at 17 g/cm² is negligible, then one can calculate the 60° zenith backward relativistic flux from the relation

$$\text{Albedo}=\frac{\text{relativistic up}}{\text{total down}+\text{up}}=\frac{n_2'n_1-n_1'n_2}{n_1^2-n_2^2},$$

where n_1' and n_2' are the observed Čerenkov efficiencies at 60° zenith angle, and n_1 and n_2 the efficiencies for the same bias at sea level. Calculated albedo values are given in the last line of the table. These data have poor statistical accuracy because of the subtraction process and insufficient data at high altitude.

The apparatus in principle gives no albedo data on nonrelativistic particles, and in its present crude form, requires two measurements differing by 180° in zenith to determine the backward flux. It appears, however, that with further development this type of detector will have a number of applications in cosmic-ray research.

Acknowledgment is made to C. L. Critchfield for the initial suggestion of applying Čerenkov radiation to this problem, and to Mr. Baskin and Mr. Mitchell for valuable assistance with the experiment.

* This work supported by the joint program of the AEC and ONR.

[1] P. A. Čerenkov, Compt. rend. acad. sci. URSS 2, 451 (1934).
[2] R. L. Mather, Phys. Rev. 84, 181 (1951).
[3] I. Frank and I. Tamm, Compt. rend. acad. sci. URSS 14, 109 (1937).
[4] J. V. Jelly, Harwell Nuclear Physics Conference (September, 1950).

A Second γ-Transition ($d_{\frac{3}{2}}\rightarrow s_{\frac{1}{2}}$) in $Xe^{129\,m}$

S. Thulin and I. Bergström
Nobel Institute for Physics, Stockholm, Sweden
(Received February 4, 1952)

EARLIER we have reported a new isomer of Xe^{129}.[1] It was found that the ratio of the intensities of the K and L conversion electrons of Xe^{129m} was close to that of Xe^{131m}, indicating

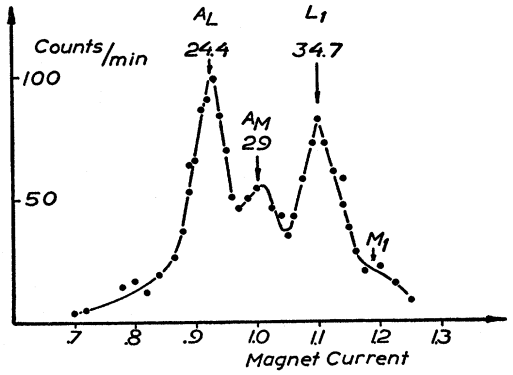

FIG. 1. Low energy electron lines of Xe^{129m}.

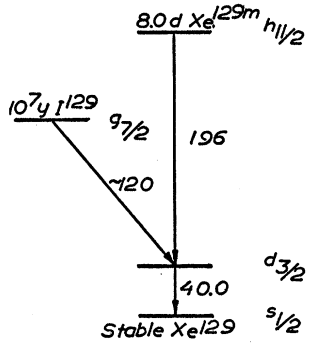

FIG. 2. Decay scheme of I^{129} and Xe^{129m}.

that the isomeric transitions are of the same type. The spins of the ground states of Xe^{129} and Xe^{131} are known to be 1/2 and 3/2 respectively. The experiments then favored the spins 9/2 and 11/2 for the isomeric states. However, the strong spin-orbit coupling model suggests the spin 11/2 also for the isomeric state of Xe^{129}. In order to obtain agreement with the theory, it is necessary to postulate a second γ-ray in the decay of Xe^{129m}. We have remeasured Xe^{129m} with a stronger sample and found a γ-ray of the energy 40.0 kev.

Figure 1 shows the low energy electron lines of an electromagnetically separated Xe^{129m} sample. In addition to the K and $L+M$ conversion lines of the 196-kev isomeric γ-ray and the two strongest Auger lines, there is a line at the energy 34.7 kev, which for the following reason must be interpreted as the L line of a 40.0-kev γ-ray. Earlier experiments[2] on Xe^{131m} have shown that the intensity ratio of the Auger lines and the isomeric K conversion line is 0.16 ± 0.02 (fluorescence yield of $Xe=0.84\pm0.02$). From Fig. 1, however, we find that this ratio is about twice the expected value. This means that Auger electrons must also be due to another K conversion line, having an intensity comparable to that of the K line (K_2) of the isomeric γ-ray. The intensity of the 34.7-kev line, however, is only ~0.15 of that of the K_2 line. It must therefore be concluded that the 34.7-kev line is an L line of a γ-ray of the energy 40.0 kev. The corresponding K line at 5.4 kev cannot be detected with the GM-window, which we used.

Borkowski and Brosi[3] have reported a 39-kev γ-ray in the decay of I^{129}. This γ-ray is certainly identical with that found by us. The decay scheme of Xe^{129m} and I^{129} is presented in Fig. 2. Thus Xe^{129m} is now in excellent agreement with the predictions of the strong spin-orbit coupling model.

It should be pointed out that we have not been able to observe the crossover transition. $E5$ radiation is thus in this case much less probable than $M4$ radiation, which is in contradiction to older theories. Hill[4] has reached similar conclusions for some of the Te isomers.

[1] I. Bergström, Nature 167, 634 (1951).
[2] I. Bergström, Arkiv. Fys. (to be published).
[3] C. J. Borkowski and A. R. Brosi, Oak Ridge National Laboratory Report No. 607 (1950).
[4] R. D. Hill, Phys. Rev. 81, 470 (1951).

Probing the Space-Charge Layer in a p-n Junction

G. L. Pearson, W. T. Read, and W. Shockley
Bell Telephone Laboratories, Murray Hill, New Jersey
(Received January 25, 1952)

ACCORDING to theory, the rectifying junctions of semiconductor art involve space-charge layers. These layers contain relatively small densities of holes and electrons and acquire their charge density from ions, donors, and acceptors. Evidence for the presence of these layers has been obtained from capacity measurements of rectifying diodes biased in the reverse

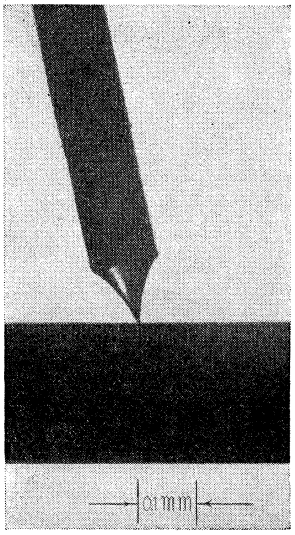

FIG. 1. Tungsten point for probing $p-n$ junctions.

directions. Schottky and his colleagues,[1] who devised the theory and made the first measurements for metal-semiconductor contacts, found that the predicted $V \propto C^{-2}$ relationship generally held.

For $p-n$ junctions with linear concentration gradients the relationship[2] should be $V \propto C^{-3}$, a prediction found to agree with experiment for many $p-n$ junctions studied.[3] If the transition from uniform n-type to uniform p-type is abrupt, the Schottky $V \propto C^{-2}$ relationship should again apply.[2] Underlying these relationships is the theory that the capacity per unit area is

$$C = K/(4\pi W), \tag{1}$$

with W the width of the space-charge layer, C the capacity per unit area, and K the dielectric constant. So far as we are aware relationship (1) has not previously been verified by direct measurement of the width W of the space-charge layer.

We have investigated the extent and potential distribution in the space-charge region in a germanium $p-n$ junction[4] by measuring the zero-current potential of a tungsten probe pressed against the space-charge layer where it comes to the surface of a specimen of square cross section cut parallel to the x-axis. The probe, a photograph of which is shown in Fig. 1, was pointed by an electrolytic etch.[5] The space-charge layer is wide compared to the area of contact of the point and may be thought of as a region of dielectric. If the point is at the natural potential of the dielectric, the voltage between the point and the semiconductor is relatively small; on the other hand if the point has a potential applied to it externally, a strong local field will be set up. Since there are relatively few holes or electrons to extract, the current which the point carries should consist predominantly of injected carriers. This is observed to be the case: with fixed voltage between the n- and p-terminals; making the point positive in respect to the floating potential results in a positive current from point to semiconductor which shows up almost entirely in an equal added current in the p-terminal lead, and mutatis mutandis the same for negative potentials. This experimental result may be taken as evidence that at the zero-current condition, the point is floating substantially at the space-charge potential. Furthermore, since the dielectric constant is 16.1, the fringing effects will be small and the potential distribution on the surface will be of nearly the same form as in the interior.

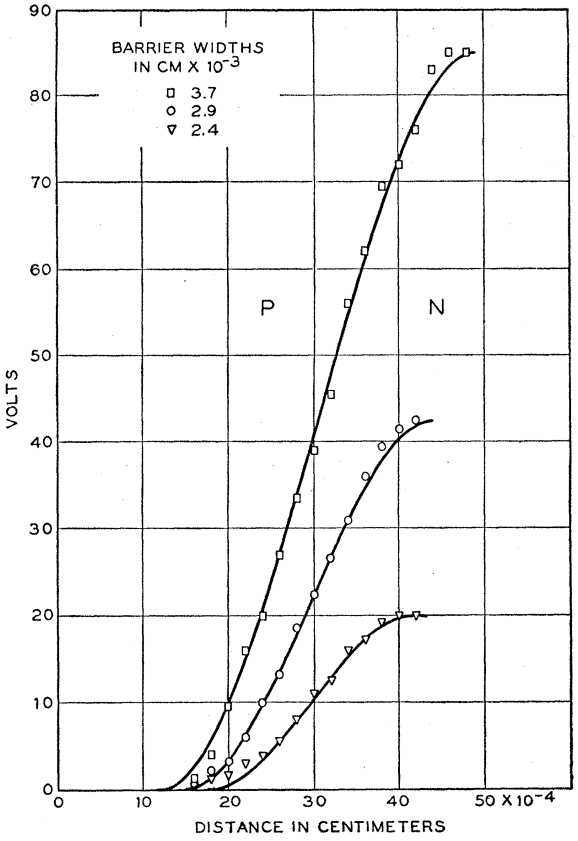

FIG. 2. Voltage *vs* distance through space-charge barrier.

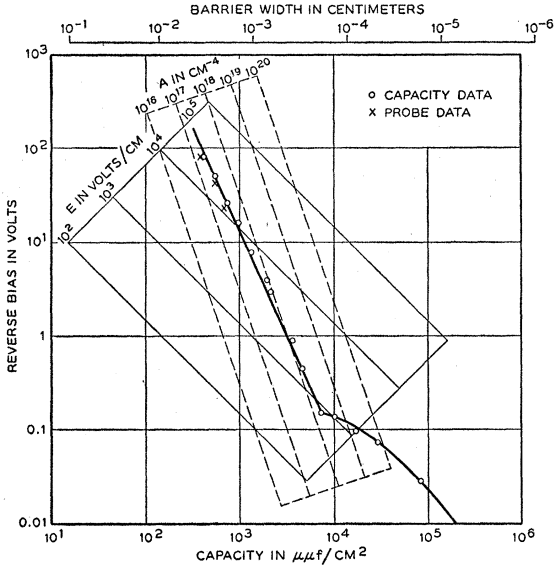

FIG. 3. Capacity and barrier width as functions of reverse bias. E =average field. A =impurity concentration gradient.

The point was moved by dragging it with light pressure in the x-direction with a Hilger interferometer movement and the zero current potentials measured as a function of distance. A typical set of data for three different potentials across the junction is shown by points in Fig. 2. Within experimental error, the same curve for 45 volts was obtained on the other three sides of the specimen.

The curves are cubics used to estimate the locations of zero-potential gradient and thus the width of the space-charge layer. The relationship (1) between W and C is tested in Fig. 3 by

plotting W *vs* V and C *vs* V, using Briggs' infrared value[6] $K=n^2=16.1$ to relate the C and W scales. On the basis of this procedure the points agree, and within this accuracy the experiment confirms that n^2 at infrared equals K at 1000 cps. Unfortunately, the junction studied has neither a linear concentration gradient nor an abrupt transition as evidenced by the approach of the data to $C \propto V^{-2}$ and in fact the curves of Fig. 2 can be equally well fitted by parabolas. This introduces an uncertainty in the W estimate of about 30 percent, which we hope to eliminate by future studies of other junctions.

We are indebted to E. Buehler, M. Sparks, and G. K. Teal, who prepared the single crystal $p-n$ junction and to W. L. Bond, P. W. Foy, and H. R. Moore for help with the measurements.

[1] W. Schottky and E. Spenke, Wiss. Veröff. Siemens-Werk. **18**, 1 (1939); see also S. J. Angello, Elec. Eng. **68**, 865 (1949).
[2] W. Shockley, Bell System Tech. J. **28**, 435 (1949).
[3] McAffee, Ryder, Shockley, and Sparks, Phys. Rev. **83**, 650 (1951); and Goucher, Pearson, Sparks, Teal, and Shockley, Phys. Rev. **81**, 637 (1951).
[4] This junction is the same as that investigated by Goucher *et al.* (reference 3).
[5] The technique employed is that of W. G. Pfann, Trans. Am. Inst. Mining and Metall. Engrs. **175**, 606 (1948).
[6] H. B. Briggs, Phys. Rev. **77**, 287 (1950).

Electron Interferometer*

L. MARTON
National Bureau of Standards, Washington, D. C.
(Received January 28, 1952)

THIS brief report contains the basic principles of an interferometer operating with electron beams. The possibility of building such an interferometer may have occurred to many, but in the absence of any publications on this subject some elementary considerations may not be misplaced.

It is rather simple to conceive an interferometer operating with electron beams based on the equivalent light optical experiment of Young. In principle, the double slit method could be employed but simple calculations, based on light optical analogies, indicate that the dimensions and complexities of such an instrument are rather undesirable. Because of the short wavelength, the source size, the size of the slits and their separation, and the separation of the fringes becomes so small that a major experimental effort may be needed for coping with them. In view of these difficulties it is worthwhile to explore the possibilities of a wide beam interferometer instead of a narrow beam instrument. In principle a wide beam interferometer of, let us say, the Michelson or the Jamin type is possible provided an efficient beam splitter is available. Such a good beam splitting mechanism exists for electrons, although not in the customary sense of light optics. Diffraction from thin crystal lamellae offers an excellent mechanism for carrying out such an interferometer experiment. Several lamellar crystals are needed in the manner indicated in Fig. 1. Let us assume an incident parallel beam of electrons passes through a thin crystal in the manner indicated by Fig. 1(a). Part of the beam is transmitted and part of it is diffracted. At a certain distance a second crystal is placed. Part of the original beam again is transmitted and part of it is diffracted as indicated. The same applies to the beam diffracted on the first crystal. The same phenomenon is repeated again on a third crystal placed at equal distance. By placing convenient limiting apertures we can select two diffracted beams out of the multitude of all the beams indicated on Fig. 1(a) and have a total path indicated on Fig. 1(b). The resulting trajectories correspond roughly to the equivalent of the Mach-Zehnder type interferometer. Figure 1(b) indicates the optical path for zero-path difference. A field gradient across the two paths will produce a path difference which can be observed by means of the shifting of the fringes localized at infinity.

To convince ourselves that the proposed scheme is feasible, we carried out light optical analog experiments. They consisted in reproducing the optical path indicated on Fig. 1(b) by means of transmission-type grating replicas. It was found that while such a system does not offer any particular advantages as compared to the conventional interferometer, it constitutes a perfectly good light optical interferometer and it helped us to compute some of the design characteristics of the electron beam instrument. Further proof for the soundness of the idea is furnished by the electron microscope observations of interference fringes published by Mitsuishi, Nagasaki, and Uyeda.[1] Similar observations have been reported also by Rees[2] from Australia and also by Hillier.[3] Observations in all three places indicate that the type of interference necessary for the operation of an electron interferometer is produced on lamellar thin crystals.

Calculations have been carried out to determine the tolerances for misalignment of the elements of an electron beam interferometer. These calculations will be reported later by J. Arol Simpson. Anticipating this report it may be mentioned that the dimensional and other tolerances of the instrument are well within experimental possibilities.

The crystals required for carrying out such experiments can be either selected from natural crystals or grown for the purpose.

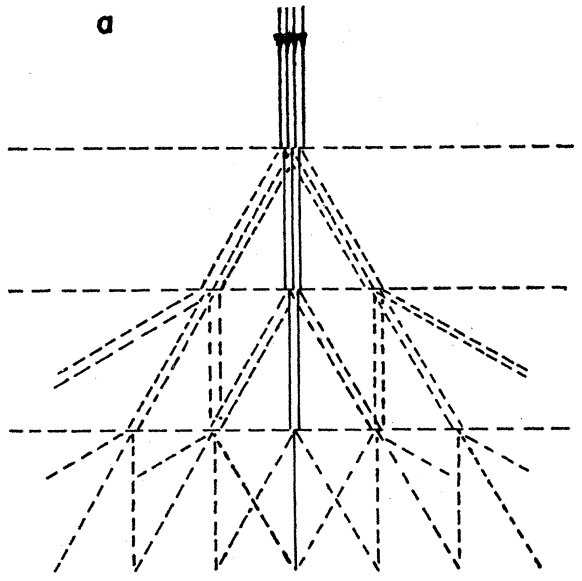

FIG. 1(a). Schematic representation of rays passing through three crystals.

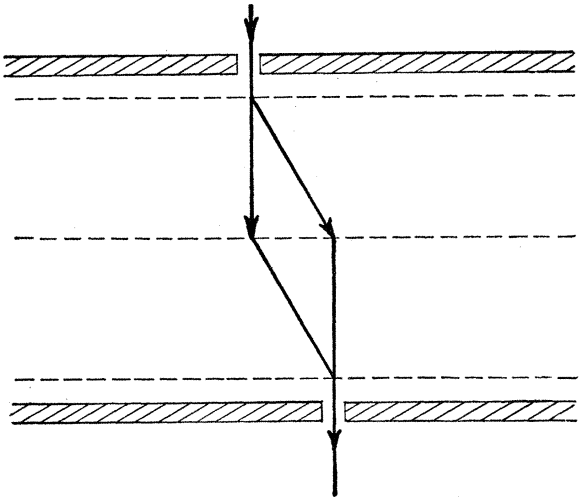

FIG. 1(b). Rays as limited by apertures.

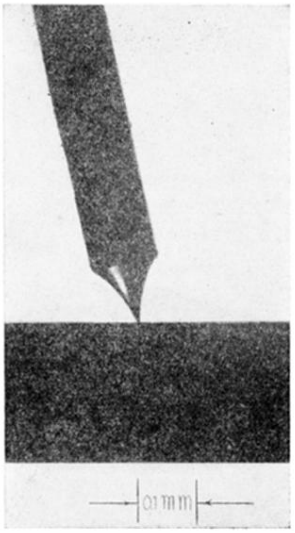

FIG. 1. Tungsten point for probing $p-n$ junctions.